Journal of Sound and Vibration (1998) **213**(1), 169–188

DEVELOPMENTS OF THE INDIRECT METHOD FOR MEASURING THE HIGH FREQUENCY DYNAMIC STIFFNESS OF RESILIENT ELEMENTS

D. J. THOMPSON

Institute of Sound and Vibration Research, University of Southampton, Highfield, Southampton SO17 1BJ, England

W. J. VAN VLIET AND J. W. VERHEIJ

TNO Institute of Applied Physics, P.O. Box 155, 2600 *AD Delft, The Netherlands*

(*Received* 13 *August* 1997, *and in final form* 7 *January* 1998)

The complex stiffness of resilient elements is an important parameter required in order to model vibration isolation for many applications. Measurement methods are being standardized which allow such a stiffness to be measured as a function of excitation frequency for known loading conditions. This paper describes one such method, the indirect method, in which the resilient element is placed between two large blocks, the vibrations of which are measured. A number of refinements to this method are proposed here. These aspects of the method are then illustrated by using example results of measurements on a resilient rail pad for use in railway track. It is shown how the frequency range of the measurements can be extended and how rotational and lateral components can be separated reliably.

1. INTRODUCTION

Resilient mounting is widely used in noise and vibration control as a means of isolating a vibration source from a receiving structure or from a structural component with a significant radiating area. Examples include the mounting of engines in vehicles, vehicle suspensions and the mounting of rails in railway tracks. The stiffness and damping of resilient elements are important parameters, required when modelling any form of resilient mounting. For example, models of railway track dynamic behaviour require numerical values for the stiffness and damping of rail pads. These are resilient elements placed between the rails and concrete sleepers on modern railway track. For vertical track dynamics the compressional stiffness of the rail pad is required, whereas if lateral track dynamics are to be modelled correctly both lateral and rotational stiffnesses are required [1, 2].

At a given frequency of excitation the ratio between force and displacement can be expressed as a complex stiffness. Of greatest interest is usually the transfer stiffness, $k_{2,1} = F_2/u_1$ (for $u_2 = 0$), that is the ratio of the force F_2 transmitted into a blocked termination (2) to the deflection u_1 input at the free termination (1). The input stiffness, $k_{1,1} = F_1/u_1$ for $u_2 = 0$ is also of relevance.

Unfortunately many resilient elements consisting of or containing viscoelastic materials have a complex stiffness which is highly dependent on parameters such as preload, temperature, frequency, strain amplitude and strain history. Furthermore, the mass of a resilient element introduces internal resonances at high frequencies which cause further

0022–460X/98/210169 + 20 $25.00/0/sv981492

frequency dependence. In this resonance region the transfer stiffness differs significantly from the input stiffness. Measurement methods are therefore required in which as many as possible of these variables are controlled whilst the stiffness is measured as a function of frequency. Moreover the resilient element usually provides a connection of finite impedance between six vibrational degrees of freedom at one side and six at the other side. Although some terms can be equal to one another or zero by symmetry considerations, to characterize a general resilient element 36 transfer stiffness terms and 21 input stiffness terms are required ($k_{1,1}$ is symmetric for linear systems by reciprocity).

An international standard is in preparation which describes measurement methods for determining the dynamic stiffness of resilient elements [3–5]. Two basic measurement methods are distinguished, referred to as the direct method and the indirect method. In the direct method the transfer stiffness is measured by using a load cell or force transducer at the blocked termination to measure F_2 and either a displacement transducer or an accelerometer to measure u_1. The excitation is often provided by a hydraulic actuator which can also generate preloads to the system. This method is used widely; see reference [6]. A second force transducer can also be used to measure F_1 allowing $k_{1,1}$ to be obtained.

The measurement rigs designed for the direct method are often limited to frequencies below typically 300 Hz. Furthermore the direct method is often limited to the axial direction, whereas other directions are generally important too. The indirect method [7, 8] has been developed as an alternative which extends the possibilities for measuring at higher frequencies and for other degrees of freedom. Here the force F_2 is not measured directly but is derived from the (relatively small) vibration u_2 of a blocking mass of known mass m_2 at the 2-side of the resilient element, by making use of Newton's second law, $F_2 = m_2 \ddot{u}_2$. This method will be described in more detail in section 2. It has previously been applied to many different types of resilient element, notably engine mounts for ship diesel engines [8], and more recently to various rail fasteners [2, 9]. In this paper, new measurements of a resilient rail pad are included to illustrate the method, and in particular a number of improvements which are proposed here. These include an extension to the method to allow lower frequency results to be obtained and a method for reliably separating lateral and rotational stiffnesses.

2. THE INDIRECT METHOD FOR MEASURING TRANSFER STIFFNESS

2.1. COMPLEX STIFFNESS MATRIX

The dynamic behaviour of a resilient element in a single direction can be described by the well known matrix relation

$$\begin{pmatrix} F_1 \\ -F_2 \end{pmatrix} = \begin{bmatrix} k_{1,1} & -k_{2,1} \\ -k_{1,2} & k_{2,2} \end{bmatrix} \begin{pmatrix} u_1 \\ u_2 \end{pmatrix}. \tag{1}$$

For the so-called blocked termination, $u_2 = 0$, it can be seen that the transfer stiffness, $k_{2,1} = F_2 / u_1$ and the input stiffness, $k_{1,1} = F_1 / u_1$, as discussed in the introduction. For linear passive elements the principle of reciprocity leads to $k_{1,2} = k_{2,1}$. If the resilient element is symmetrical between 1 and 2, $k_{1,1} = k_{2,2}$. In the case of a massless spring $k_{1,1} = k_{1,2}$ and $F_1 = F_2$. At low frequencies the massless damped spring is a good approximation to most resilient elements, but at high frequencies the mass of the element causes standing waves to occur within resilient elements. For more general linear passive elements the above equalities (apart from the principle of reciprocity) do not apply.

Equation (1) can be extended to a multi-degree-of-freedom situation by writing F_i and u_i as column vectors each with six elements and the stiffness matrix, K, as partitioned into four 6×6 matrices.

2.2. MEASUREMENT APPARATUS

The measurement apparatus used for the indirect method is shown schematically in Figure 1. It consists of two blocks of known mass between which the resilient element is mounted. This whole arrangement is itself mounted on very soft rubber springs under the lower block and a hydraulic preload is applied through further soft isolators to the upper block.

The large mass of the lower block gives it a much higher impedance than the resilient element which serves to satisfy the requirement that $|u_2| \ll |u_1|$. Under this approximation, equation (1) reduces to

$$F_2 \approx k_{2,1}\, u_1. \tag{2}$$

The high frequency vibration of the upper block is introduced by using electrodynamic exciters. Accelerometers are used to measure the vibration of both blocks in terms of their accelerations $\ddot{u}_1$ and $\ddot{u}_2$.

Figure 1 also shows the measurement apparatus approximated as a mass–spring system. For simplicity only the axial direction is considered. The element under test has a complex frequency-dependent stiffness matrix K_p, the upper and lower blocks have masses m_1 and m_2, respectively, and rest on further resilient elements of input stiffness k_1 and k_2

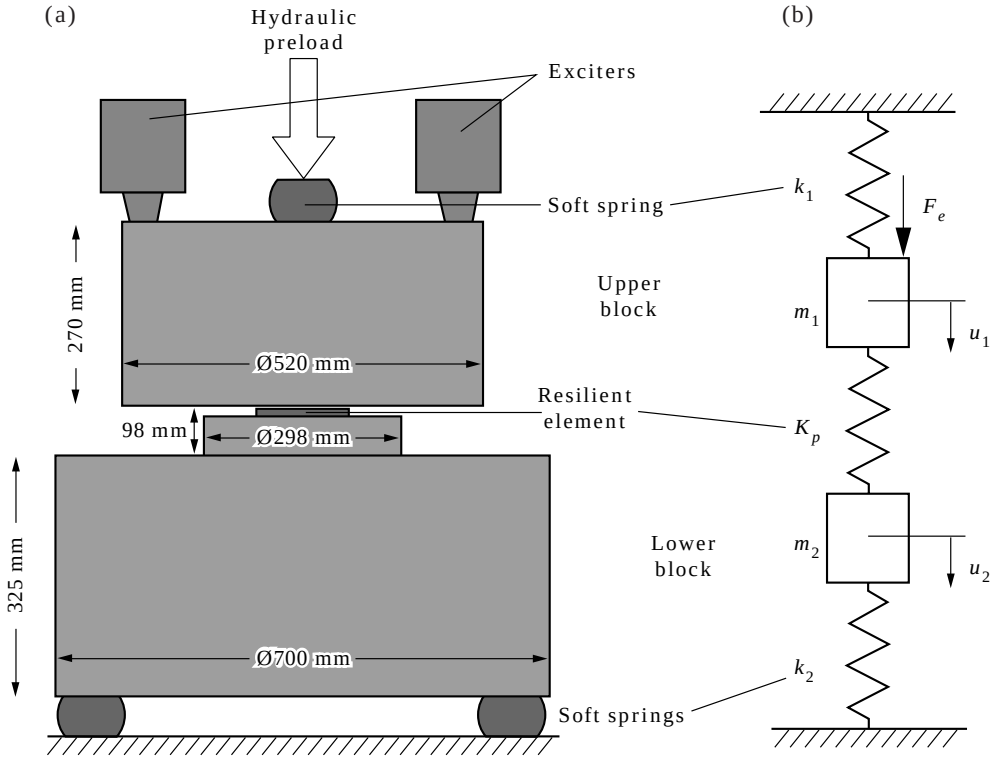

Figure 1. (a) Schematic diagram of the measurement apparatus (not to scale), showing main dimensions. (b) Equivalent mass–spring system.

respectively. These are assumed to be grounded at the other end as they are sufficiently soft and the structure on which they rest has a sufficiently high impedance. The stiffness of these resilient mounts has to be chosen to be low enough to minimize any effect on the impedance of the blocks for the frequency range under consideration: i.e., the resonance frequency of m_i on k_i has to be significantly lower than the lowest measurement frequency. If this is not the case, a correction has to be applied, as discussed in section 5. Conversely, the stiffness must be high enough to provide a stable measurement arrangement even under the significant preloads. Distribution of the springs around the perimeter of the lower block helps to achieve this. In general, k_1 and k_2 should be softer than the elements of K_p, preferably by at least an order of magnitude. They should also not stiffen too much under preload.

The preload is not modelled explicitly here although it has an effect on the dynamic values of K_p, k_1 and k_2. The excitation of the upper block has the effect of introducing the vibration amplitude u_1, which can be measured. The usual measurement method consists of determining u_1 and u_2 as a function of frequency, by measuring the transfer function between them.

2.3. EQUATIONS OF MOTION

The equations of motion of this two-degree-of-freedom system under the influence of a harmonic force $F_e\,e^{i\omega t}$ applied to the upper block, can be written as

$$k_1\,u_1 + k_{p1,1}\,u_1 - k_{p1,2}\,u_2 - \omega^2 m_1\,u_1 = F_e, \tag{3}$$

$$k_2\,u_2 + k_{p2,1}\,u_1 + k_{p2,2}\,u_2 - \omega^2 m_2\,u_2 = 0, \tag{4}$$

where u_i now represents the amplitude of harmonic vibration of block i. These equations can be solved to give two resonance frequencies:

$$\begin{vmatrix} k_{p1,1} + k_1 - m_1\,\omega^2 & -k_{p1,2} \\ -k_{p2,1} & k_{p2,2} + k_2 - m_2\,\omega^2 \end{vmatrix} = 0. \tag{5}$$

For frequencies which are sufficiently low that $k_p = k_{p1,1} = k_{p1,2}$ etc., and that the various stiffnesses are effectively independent of frequency and for the required condition that $k_1 \ll k_p$ and $k_2 \ll k_p$, this reduces to

$$\omega_1 \approx \sqrt{(k_1 + k_2)/(m_1 + m_2)} \tag{6}$$

and

$$\omega_2 \approx \sqrt{k_p\,(m_1 + m_2)/m_1\,m_2}. \tag{7}$$

For a given force excitation, therefore, the responses u_1/F_e and u_2/F_e will have maxima at these resonance frequencies. However, the force F_e itself is not measured in this method. Rewriting equation (4) gives

$$u_2/u_1 = k_{p2,1}/(k_2 + k_{p2,2} - m_2\,\omega^2). \tag{8}$$

The transfer function between u_2 and u_1 (or equivalently between the corresponding accelerations) thus has a peak where

$$\omega_2' = \sqrt{(k_2 + k_{p2,2})/m_2}. \tag{9}$$

Although this is not a system resonance as such, it is equivalent to the resonance of the lower block on the two springs k_2 and $k_{p2,2}$, with the upper block held rigidly. For

sufficiently high frequencies, ω above about $3\omega_2'$, the denominator of equation (8) can be approximated by $-m_2\,\omega^2$. The stiffness can then be derived as:

$$k_{p2,1} \approx -m_2\,\omega^2(u_2/u_1) \qquad \text{for } \omega > 3\omega_2'. \tag{10}$$

This is the basis of measurements reported in references [7–9].

3. EXAMPLE MEASUREMENT RESULTS

3.1. RESILIENT ELEMENTS TESTED

Measurements are presented which have been carried out according to the above method on a series of rail pads. These results have also been quoted by Fenander [10]. They are included here to illustrate the method and the advantages gained by the improvements presented in later sections.

The rail pads measured are Pandrol type 5877 studded rubber pads, nominally 10 mm thick, with maximum dimensions 194×160 mm. The area covered by the studs is 154 mm wide in each direction. These are the normal pads used in Sweden and similar pads are in use for example in the U.K., Belgium, Norway and Finland. Four nominally identical pads have been measured, but the results presented here are only for one of these (for others see reference [10]). The samples supplied were in new condition.

3.2. DETAILS OF MEASUREMENT APPARATUS

For use with the measurement apparatus, a series of blocks is available, mostly cylindrical, which can be used as either m_1 or m_2. Different blocks are chosen according to the expected stiffness, the required frequency range and any geometrical constraints. For the current measurements, the upper block consisted of a solid steel cylinder of diameter 0·520 m, height 0·270 m and mass 450 kg. Although the mass of this block is of little importance, the diameter and stiffness were required to spread the excitation from two exciters and the height was required to allow the measurements of lateral and rotational stiffnesses discussed in section 6.

The lower block comprised a steel cylinder of diameter 0·700 m and height 0·325 m. On the underside of the lower block, a series of concentric holes had previously been made, reducing the mass by approximately 65 kg and raising the centre of mass slightly. An aluminium spacing block was fixed to the centre of the upper side of the block, using a very hard adhesive. This was 0·098 m high, with a diameter of 0·298 m and a mass of 18 kg. Its purpose was to increase accessibility between the two blocks (for transducers, etc.). It can also reduce any possible excitation of the lower block by the airborne path which exists in parallel to the path via the resilient element, although this is unlikely to be relevant for resilient elements of the stiffness measured here. The total mass of the lower block was measured as 930 kg.

Both bearing surfaces were smooth and free from holes or other defects. The preload is measured by using a load cell; the actual preload is this load plus the weight of the upper block, that is 450 kg or 4·4 kN. The excitation signal was a rapidly swept sine (“chirp”) covering the frequency range of the measurement, with a period of 1 s. Two exciters are used, symmetrically placed with respect to the central hydraulic preload, in order to ensure a purely vertical excitation. In another test rig, used for the measurements reported in reference [9], a single exciter is placed centrally whereas the preload is applied at either side. These methods are equivalent.

In order to measure purely translational components, pairs of accelerometers were used

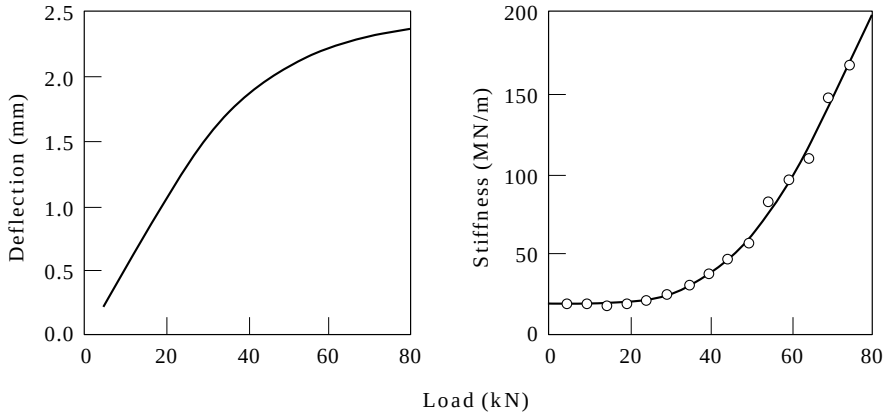

Figure 2. Static load-deflection curve (left) and incremental stiffness derived from it (right).

on each block with an analogue summation/subtraction device. This can also be used to give the difference signal, which is used when measuring rotational components.

3.3. STATIC STIFFNESS MEASUREMENTS

Although the test rig described is intended for high frequency dynamic stiffness measurements, it is also possible to use the rig to measure the static load-deflection curves. This was performed by applying the hydraulic preload in steps of 5 kN from 4·4 kN (i.e., the weight of the upper block with no hydraulic preload) to almost 80 kN. The relative deflection on either side of the block was measured by using a dial gauge, which gave readings to the nearest 10 μm.

The static load-deflection curve is shown in Figure 2. Also in this figure, the incremental static stiffness is shown as a function of preload. The static stiffness can be seen to be relatively constant (20 MN/m) at preloads up to about 25 kN, above which it increases sharply. Values of the static stiffness at the preloads used in the high frequency measurements are given in Table 1. Note that the static stiffness measurements are less reliable at high preloads as the deflection increases rather slowly as a function of load here.

3.4. CHECK OF DYNAMIC STIFFNESS FROM SYSTEM RESONANCES

For dynamic excitation, the power spectrum of the acceleration of the upper block is shown in Figure 3 for the five preloads. This equals the spectral density due to the use of 1 Hz frequency spacing in the analysis. The overall r.m.s. acceleration level of the upper block, derived from the sum over this spectrum, is 0·3 m/s^2. Although the force has not

TABLE 1

Estimate of static incremental stiffnesses (from Figure 2) and of dynamic stiffness magnitudes at single frequencies estimated from the resonance frequency in Figure 3 and equation (7); total r.m.s. strain amplitudes are also listed, from Figure 4

Preload (kN)	20	30	40	60	80
Static stiffness MN/m	19	25	37	95	c. 200
Frequency f_2 (Hz)	74	84	106	166	245
Stiffness (MN/m) at f_2 (Hz)	65	85	135	330	720
Dynamic/static stiffness ratio	3·4	3·4	3·6	3·5	3·6
r.m.s. strain amplitude	85×10^{-6}	70×10^{-6}	45×10^{-6}	20×10^{-6}	9×10^{-6}

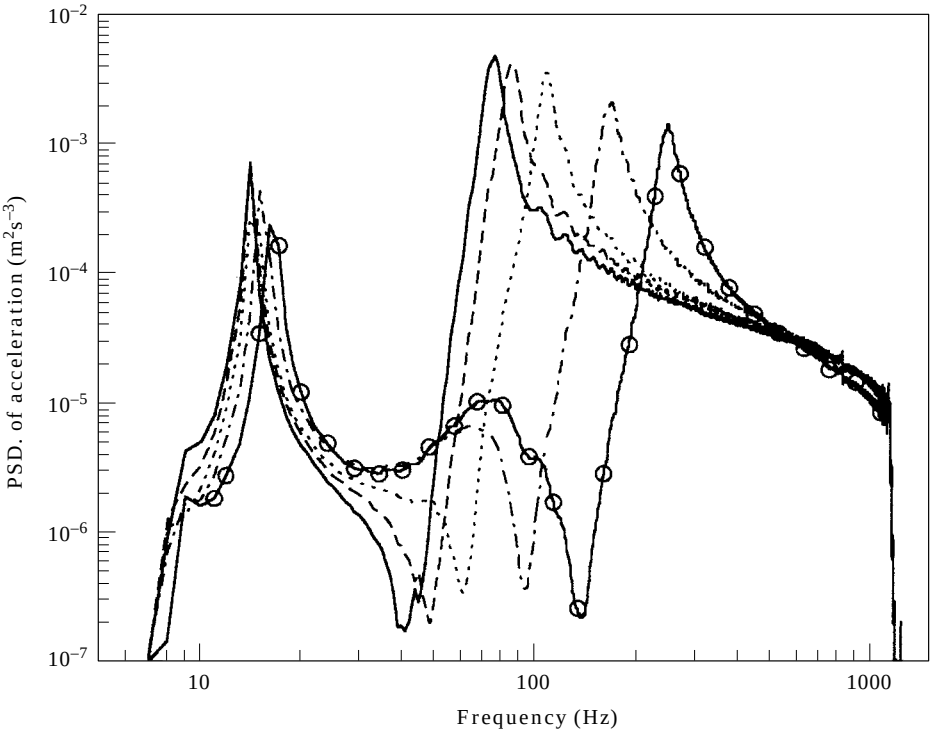

Figure 3. PSD of acceleration of upper block at various preloads (——, 20 kN; - - -, 30 kN; · · · · · ·, 40 kN; - · - · -, 60 kN; ○——○, 80 kN).

been measured, it is likely to be reasonably flat over the frequency range at least from 50 Hz to 1 kHz.

The response curves reveal two resonances of the system. These are ω_1 and ω_2 as discussed in section 2.3. The first, between 14 and 16·5 Hz, corresponds to the complete mass of the test rig $m_1 + m_2$ vibrating on the combined stiffness of the upper and lower foundations $k_1 + k_2$, see equation (6). This is relatively insensitive to the preload. Given the combined mass of 930 + 450 kg, the stiffness $k_1 + k_2$ can be estimated as increasing from about 10 to about 15 MN/m under the effect of the preload. The second resonance at $f_2\,(=\omega_2/2\pi)$ corresponds to the two masses moving in anti-phase on the resilient element (the rail pad), see equation (7). Provided that $k_p \gg k_1 + k_2$, these frequencies allow a first estimate of the dynamic stiffnesses of the rail pad, as listed in Table 1. Upon comparing these dynamic stiffnesses with the static stiffnesses at the same preload, it emerges that the ratio between them for this pad is virtually constant at 3·5 for all preloads.

Figure 4 shows the power spectral density of the strain in the rail pad. This has been derived from a direct measurement of $u_1 - u_2$ obtained using a further summation/subtraction device to combine the signals of u_1 and u_2. With the data below 10 Hz which are contaminated by noise being ignored, the r.m.s. strain amplitudes calculated from these spectra have been derived, and are listed in Table 1.

3.5. MEASUREMENT OF DYNAMIC STIFFNESS

The stiffness derived by using the transfer function u_2/u_1 according to equation (10) is given in Figure 5. These "stiffnesses" contain a peak at the frequency f_2' $(=\omega_2'/2\pi$, see equations (8) and (9)), at which the phase also deviates significantly from the typical values.

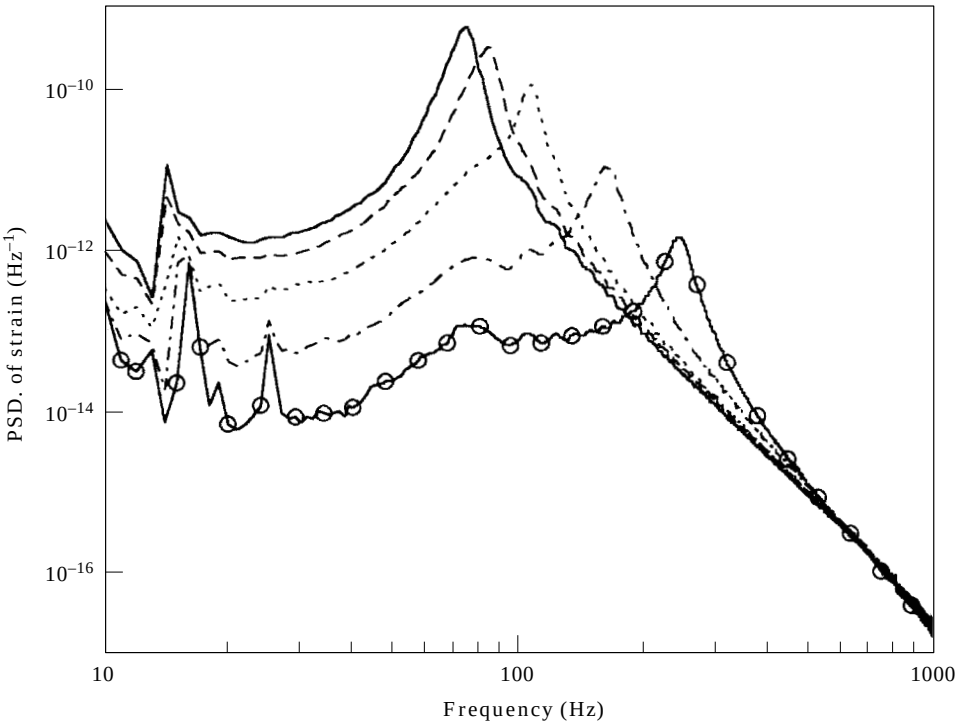

Figure 4. PSD of strain in pad and various preloads. Key as Figure 3.

The corresponding "resonance" frequency increases with increasing preload. Table 2 lists these frequencies, and the stiffness values derived from equation (9) by assuming $k_p \gg k_2$ (in section 4.2 below, k_2 is shown to be between 6 and 9 MN/m depending on preload; the values listed at f_2' are actually $k_p + k_2$, and so give a slight overestimate of k_p). The values are, of course, similar to those listed in Table 1 which were derived from f_2.

The values derived from the resonance frequencies can be used to check the results of the actual measurement method at discrete frequencies, as they are immune from any calibration error. Such errors are always a possibility, no matter how slight, in transfer function measurements. Therefore Table 2 also lists the stiffness values measured from the curves of Figure 5 at the lower limiting frequencies, $3f_2'$. These are similar to those implied from the resonance frequency itself. Above these frequencies, the stiffness can be seen in Figure 5 to increase slightly with frequency.

4. EXTENSION TO THE METHOD TO ALLOW MEASUREMENTS AT LOWER FREQUENCIES

4.1. REVISED EVALUATION METHOD

The procedure described above, in which the stiffness is derived from the transfer function u_2/u_1 has been used extensively to obtain high frequency dynamic stiffnesses and the draft ISO standard in reference [5] is based on this approach. However, the condition $\omega > 3\omega_2'$ introduces a rather strict limit on the lower bound of the valid frequency range. In the example measurements described above, f_2' is between 40 and 140 Hz, depending on the preload, which means that the lower limit of validity is between 120 and 420 Hz.

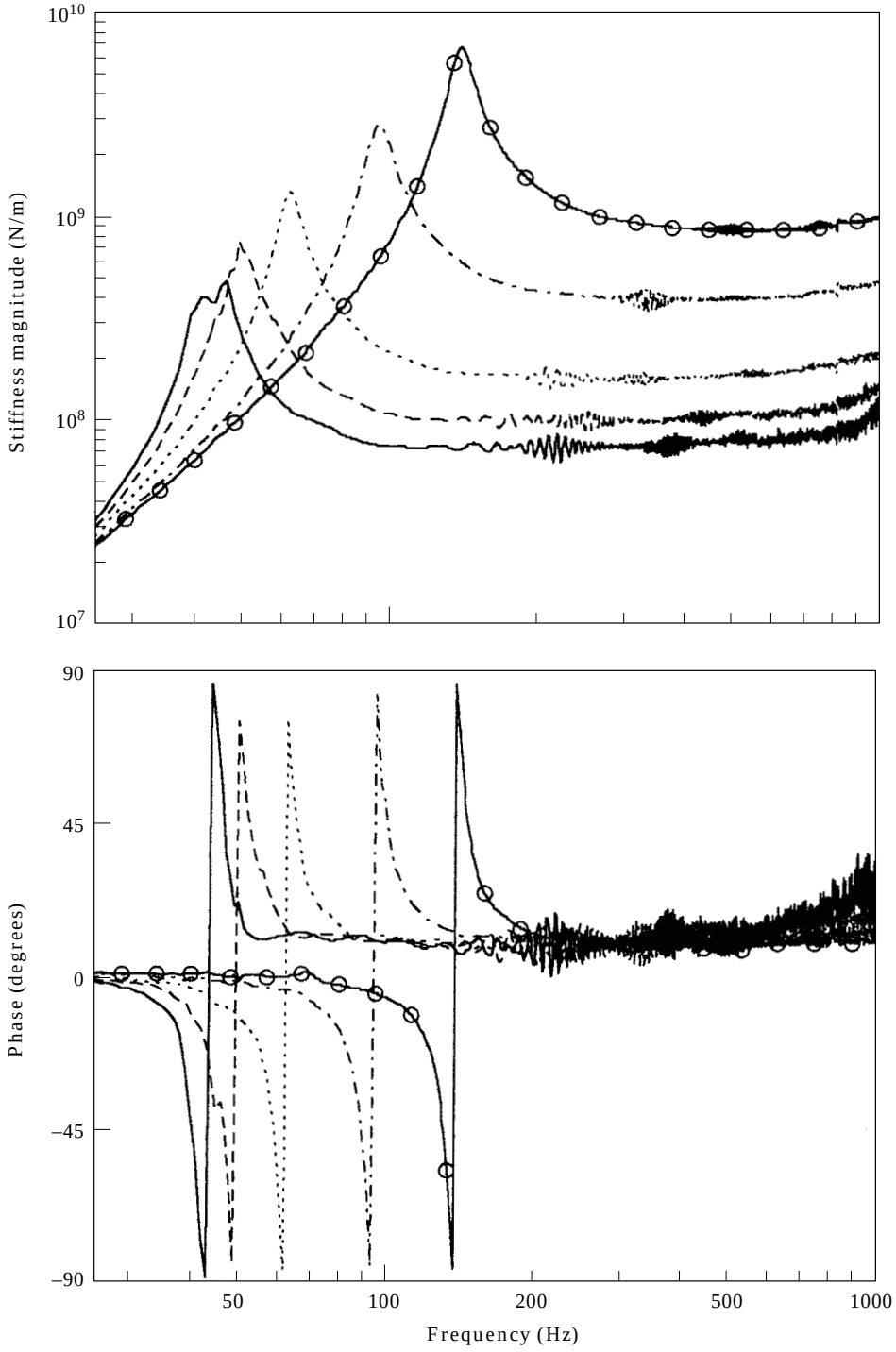

Figure 5. Magnitude and phase of complex "stiffness" measured using u_2/u_1 for various preloads. Key as Figure 3.

TABLE 2

Estimate of dynamic stiffness at single frequencies using "resonance" frequency in Figure 5 *and equation* (9), *and directly at lower limit of validity of equation* (10)

Preload (kN)	20	30	40	60	80
Frequency f_2' (Hz)	43	49	62	94	138
Stiffness (MN/m) at f_2' (Hz)	69	88	142	325	700
Stiffness (MN/m) at $3f_2'$ (Hz)	73	100	163	390	860

Investigations have therefore been carried out into extending the usual method by measuring directly the compression of the resilient element $(u_1 - u_2)$ as well as the response of the lower block u_2. This allows the lower limit of the measurement to be extended to below f_2', the aim being to measure at least down to 50 Hz. On the other hand, this is valid only if $k_p = k_{p2,1} = k_{p2,2}$ in the low frequency region in which $|u_2| \ll |u_1|$ does not hold. This will usually be the case.

The transfer function to be measured is now $u_2/(u_1–u_2)$. Equation (4) can be rewritten as

$$k_{p2,1} = \left(\frac{u_2}{u_1 - u_2}\right)((k_2 - m_2\,\omega^2) + (k_{p2,2} - k_{p2,1})). \tag{11}$$

At low frequencies, the last term vanishes; at high frequencies it is in any case much smaller than $m_2\,\omega^2$. The stiffness $k_{p2,1}$ can thus be derived from

$$k_{p2,1} \approx -m_2\,\omega^2\left(\frac{u_2}{u_1 - u_2}\right) \qquad \text{for } \omega > 3\omega_1', \tag{12}$$

where the lower limit is now given in terms of:

$$\omega_1' = \sqrt{k_2/m_2}, \tag{13}$$

which is the resonance of the lower block on its resilient mounts. This condition can also be relaxed further by applying the effective mass correction discussed below.

4.2. RESULTS OF REVISED METHOD

Figure 6 shows the results of the revised method, which also include a running average over 11 Hz to smooth the data. Compared to those in Figure 5, these results show a stiffness behaviour over a much wider frequency range, even where the strain has a "resonance".

Here only the results with coherence greater than 0·95 are presented. This limits the frequency range somewhat, but as will be discussed later, additional measurements are available for the high frequency part of the measurement range with better signal-to-noise ratios.

Not shown in these results, but noteworthy, is that the "stiffness" measured in this way has a "resonance" peak at between 13 and 16 Hz (increasing with preload). This is the frequency ω_1' given in equation (13). This means that, from equation (12), the revised method can be used from about 40–50 Hz upwards. For a mass m_2 of 930 kg, this value of ω_1' allows the stiffness k_2 to be deduced as 6 MN/m at 20 kN preload increasing to about 9 MN/m at 80 kN preload.

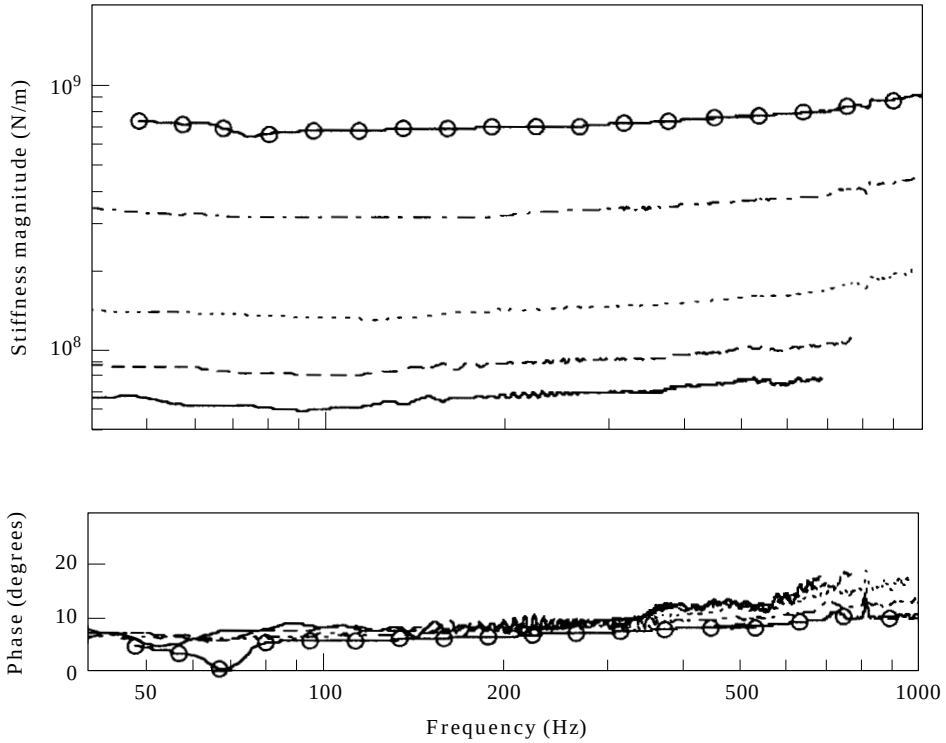

Figure 6. Magnitude and phase of complex stiffness measured using $(u_1 - u_2)/u_1$ for various preloads. Key as Figure 3.

5. CORRECTIONS FOR MASS OF LOWER BLOCK

5.1. CALIBRATION MEASUREMENTS

To allow measurements to be carried out to frequencies which are as low as possible, the mass of the lower block m_2 must be large, see equations (9, 10) and (12, 13). This mass m_2 can be measured on a balance. At very high frequencies, however, the lower block will no longer act as a rigid mass, but will exhibit resonant behaviour. Large blocks have the disadvantage that this behaviour occurs at lower frequencies than for small blocks. For a given mass, the ideal block shape is cylindrical with height equal to the diameter [5], as this maintains its constant mass character as long as possible.

It is also possible to calibrate the block to determine its effective mass as a function of frequency. To do this, the response of the lower block is determined at the positions used in the stiffness measurements when a known force is applied at the centre of the upper surface, that is the location of the resilient element during the stiffness measurements. As well as eliminating the effect of the onset of resonant behaviour at high frequencies, this effective mass measurement can also allow for the term k_2 in equations (8) or (11):

$$m_{eff}(\omega) = m_2 - k_2/\omega^2. \tag{14}$$

Note, however, that the procedure used for determining m_{eff} does not account for the stiffening of k_2 due to introduction of the preload, because it is carried out without the resilient element and therefore without the preload present in the apparatus.

Example measurement results are shown in Figure 7 in the form of the logarithmic ratio, $\Delta L_m = 20 \log_{10} (m_{eff}/m_2)$, where $m_2 = 930$ kg is the measured mass of the block. It can be seen that ΔL_m is within the range $\pm 0{\cdot}5$ dB for frequencies 70–800 Hz. At 1000 Hz, ΔL_m is $+0{\cdot}8$ dB as the block begins to show non-rigid behaviour, and at low frequencies it reduces to -1 dB at 50 Hz as the effect of the foundation resonance becomes evident. The frequency f_1' $(=\omega_1'/2\pi)$, the dip in the effective mass, occurs at about 12 Hz in this unloaded situation, which gives k_2 as about 5·5 MN/m. Also shown in Figure 7 is the effective mass calculated by using equation (14) with this value of k_2, which is very close to the measured curve.

5.2. RESULTS INCLUDING MASS CORRECTION

Upon introducing the mass correction from Figure 7, the results are produced which are given in Figure 8. The upper figure gives the magnitude of the stiffness and the lower figure the phase angle. The mass correction used is the analytical result up to 350 Hz, that is equation (14) making use of the preload-dependent values of k_2, and above that the high frequency measurement. The difference between these results and those without mass correction is less than 1 dB in the frequency range shown (see Figure 7), but is more significant below 40 Hz. This difference, although small in the frequency range of interest, is of the same order of magnitude as the frequency-dependence of the stiffness at low frequencies which would otherwise be masked.

Additionally, the high frequency results have been supplemented by the results obtained when using a more limited frequency sweep (from 380 to 1200 Hz). This reduces the excitation of the resonances ω_1 and ω_2 seen in Figure 3, and allows a more sensitive setting to be chosen on the pre-amplifier, thus reducing the instrumentation noise level and allowing an improved signal to be recorded at the higher frequencies.

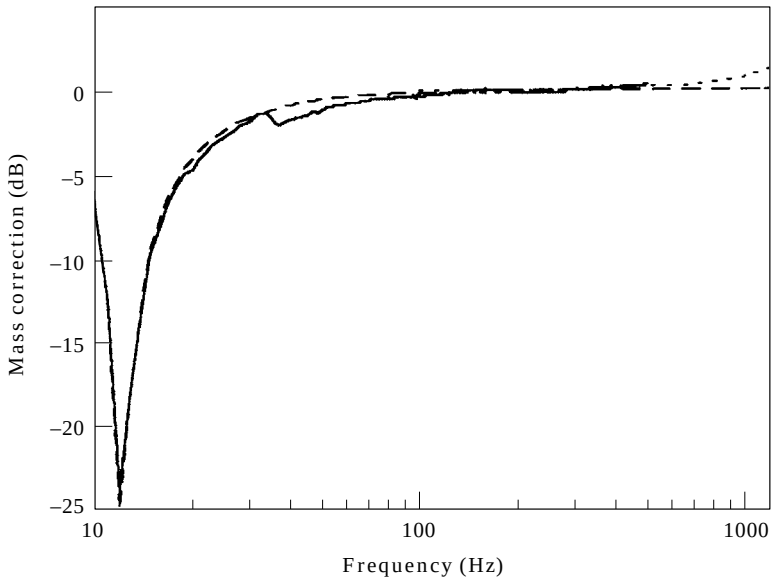

Figure 7. Correction for effective mass, $\Delta L_m = 20 \log_{10} (m_{eff}/m_2)$. Measured, —— and · · · · · ·, and estimated from equation (14), - - -.

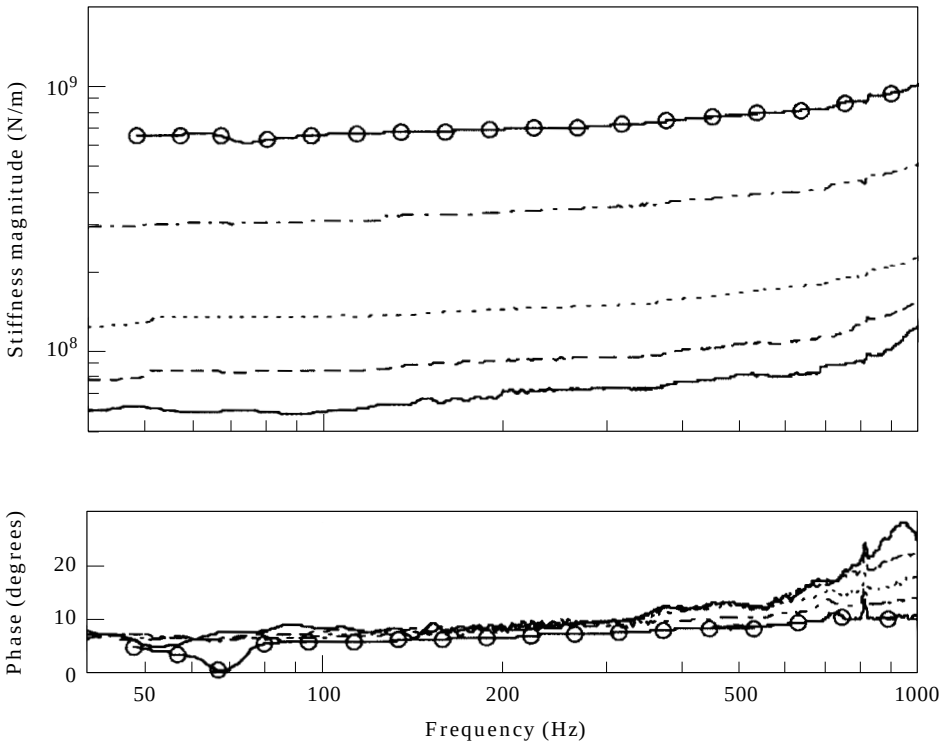

Figure 8. Magnitude and phase of complex stiffness measured using $(u_1 - u_2)/u_1$ with mass correction for various preloads. Key as Figure 3.

6. SEPARATION OF ROTATION AND LATERAL COMPONENTS

6.1. RELATION BETWEEN REQUIRED AND MEASURED QUANTITIES

In order to measure the stiffness of the resilient element to rotation about a horizontal axis, it is necessary to perform two experiments each containing a combination of lateral and rotational motion. This follows from the fact that the upper block in the test rig cannot be made to move in only the rotational degree of freedom (it always contains some translational component), and that it is not possible to measure only the moment acting on the lower block in the absence of lateral forces. The lateral stiffness can also be extracted from these measurements. To derive the lateral stiffness from a single experiment would similarly require an experiment with purely lateral motion of the upper block which is also difficult to arrange. A method has been developed to separate these two components from the two combined measurements. In preliminary form it has been proposed for inclusion in the draft standard in reference [5].

Figure 9 shows the geometry of the lateral/rotational experiments. In each experiment both the lateral translation, u, and the rotation, θ, of the upper and lower blocks are measured, using the sum and difference of the outputs from two accelerometers. The sum of the two transducer signals u_i^a and u_i^b from block i divided by 2 gives the translation at the midpoint of their locations, u_i', whilst the difference signal divided by the separation d_i gives the rotation, θ_i.

For a situation in which the lower mass effectively blocks the motion of the lower side of the resilient element, $|u_2| \ll |u_1|$ and $|\theta_2| \ll |\theta_1|$, the following four transfer stiffnesses determine the response:

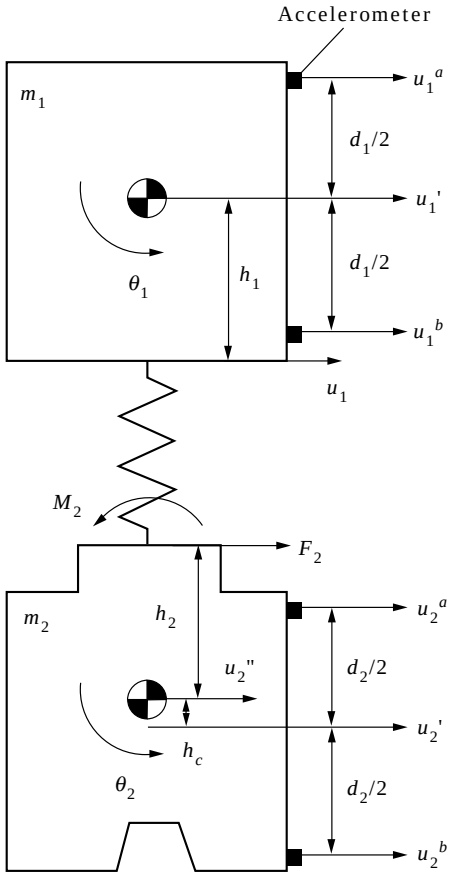

Figure 9. Schematic diagram of the measurement geometry for lateral/rotational measurements.

$$\begin{pmatrix} F_2 \\ M_2 \end{pmatrix} = \begin{bmatrix} k_{F,u} & k_{F,\theta} \\ k_{M,u} & k_{M,\theta} \end{bmatrix} \begin{pmatrix} u_1 \\ \theta_1 \end{pmatrix}. \tag{15}$$

Here u_1 and θ_1 are the displacement and rotation at the upper surface of the resilient element and F_2 and M_2 are the force and moment acting on the upper surface of the lower block. The measurements, however, consist of transfer functions between the translations u_1' and u_2' at the mean transducer positions, the rotations θ_1 and θ_2 and a reference channel. The rotation is independent of the height, but the translation depends on the height. For the reference channel, the rotation θ_1 is chosen. The required quantities can be expressed in terms of the measured quantities as

$$u_1/\theta_1 = (u_1'/\theta_1) + h_1, \tag{16}$$

where h_1 is the distance from the mean measurement position on the upper block to its lower surface, and

$$\frac{F_2}{\theta_1} = -\omega^2 m_2 \left(\frac{u_2'}{\theta_1} - h_c \frac{\theta_2}{\theta_1} \right), \tag{17}$$

$$\frac{M_2}{\theta_1} = -\omega^2 \left(m_2 h_2 \frac{u_2'}{\theta_1} + (I_2 - m_2 h_2 h_c) \frac{\theta_2}{\theta_1} \right), \tag{18}$$

where h_2 is the distance between the centre of mass of the lower block and its upper surface, and h_c is the height of the mean measurement position on the lower block below its centre of mass (see Figure 9). I_2 is the moment of inertia of the lower block with respect to rotation about its centre of mass.

6.2. EXPERIMENTAL APPLICATION

In order to solve equation (15) for the four unknown stiffnesses, two measurements are performed with different ratios of u_1/θ_1. For these, the upper block is excited laterally, first near its upper edge and then near its lower edge. With these two experiments denoted by the indices $^{(1)}$ and $^{(2)}$, equation (15) becomes

$$\begin{bmatrix} (F_2/\theta_1)^{(1)} & (F_2/\theta_1)^{(2)} \\ (M_2/\theta_1)^{(1)} & (M_2/\theta_1)^{(2)} \end{bmatrix} = \begin{bmatrix} k_{F,u} & k_{F,\theta} \\ k_{M,u} & k_{M,\theta} \end{bmatrix} \begin{bmatrix} (u_1/\theta_1)^{(1)} & (u_1/\theta_1)^{(2)} \\ 1 & 1 \end{bmatrix}. \tag{19}$$

Transposing and inverting gives

$$\begin{bmatrix} k_{F,u} & k_{M,u} \\ k_{F,\theta} & k_{M,\theta} \end{bmatrix} = \begin{bmatrix} (u_1/\theta_1)^{(1)} & 1 \\ (u_1/\theta_1)^{(2)} & 1 \end{bmatrix}^{-1} \begin{bmatrix} (F_2/\theta_1)^{(1)} & (M_2/\theta_1)^{(1)} \\ (F_2/\theta_1)^{(2)} & (M_2/\theta_1)^{(2)} \end{bmatrix}, \tag{20}$$

where the right-hand side can be expressed in terms of measured quantities by using equations (16), (17) and (18). The accuracy of this solution depends, amongst other things, on the condition number of the matrix which has to be inverted:

$$\operatorname{cond} \begin{bmatrix} (u_1/\theta_1)^{(1)} & 1 \\ (u_1/\theta_1)^{(2)} & 1 \end{bmatrix}. \tag{21}$$

A matrix with a high condition number tends to magnify errors in the measured right-hand side quantities. If u_1 had been used as the reference instead of θ_1, this condition number would have been

$$\operatorname{cond} \begin{bmatrix} 1 & (\theta_1/u_1)^{(1)} \\ 1 & (\theta_1/u_1)^{(2)} \end{bmatrix}. \tag{22}$$

From the experimental results it is found that the condition number in equation (21) is less than 5 in the relevant frequency range whereas that in equation (22) is around 9, as shown in Figure 10. Consequently the use of the rotation as the reference signal gives a more reliable inversion. Another reason for using θ_1 is that u_1 is not measured directly but reconstructed from u_1' and θ_1 (see equation (16)) making it a less reliable reference.

6.3. CALIBRATION MEASUREMENTS

The above procedure relies on the accurate knowledge of the values of a number of parameters. The separation of the accelerometers was $d_1 = 0{\cdot}250$ m and $d_2 = 0{\cdot}304$ m and by symmetry $h_1 = 0{\cdot}135$ m. The mass of the lower block, m_2, has already been determined as 930 kg and its moment of inertia, I_2, can be estimated from its dimensions as 37·9 kg m^2. According to this calculation, the centre of mass should be located at $h_c = 0{\cdot}012$ m above the centre of the steel cylindrical block. The two transverse accelerometers were located symmetrically with respect to this block, so the sum of their signals should represent the

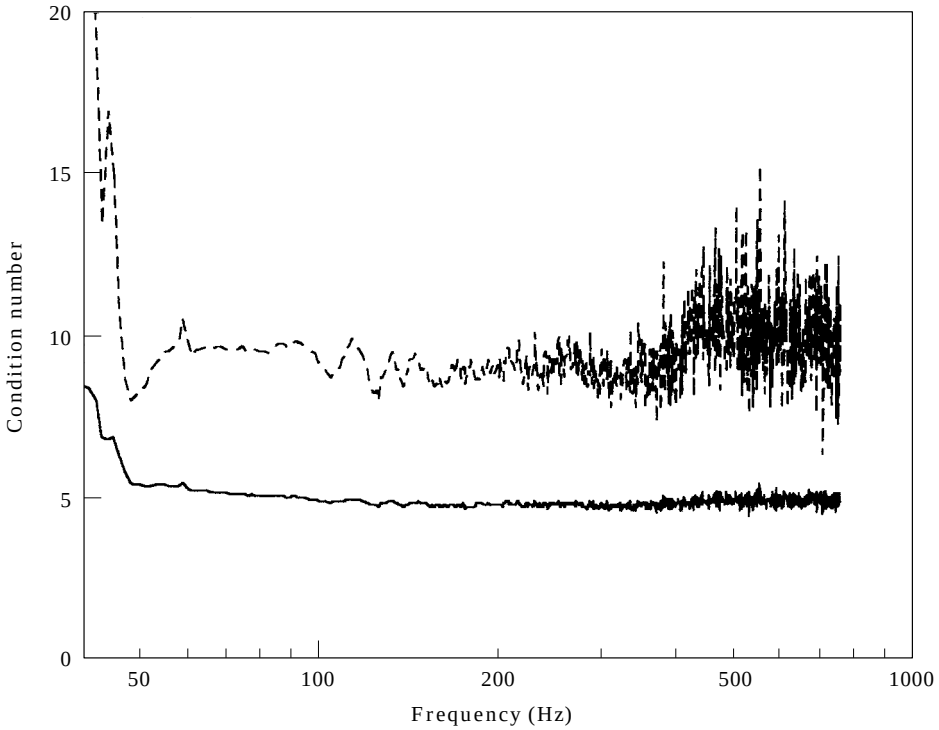

Figure 10. Condition number of measured matrices. ——, Equation (21); - - -, equation (22).

lateral vibration at its centre. From the dimensions of the blocks, the height $h_2 + h_c$ can be deduced as 0·2605 m.

To check these values, a calibration measurement has been carried out, similar to that for the effective mass in section 5.1. The block was excited laterally with a hammer about 1–2 cm below the top of the aluminium block and the response of the lower block in the lateral and rotational directions was measured. From the transfer function between the lateral force and the lateral response, the effective mass can be checked, by using equation (17). However, the mass found initially was slightly higher than 930 kg, due to the fact that the lateral response measured, u_2', is located slightly below the centre of mass. The true response of the centre of mass is given by

$$u_2'' = u_2' - h_c\,\theta_2, \tag{23}$$

which allows h_c to be deduced. The value $h_c \approx 0{\cdot}016$ m is found to be consistent with $m_2 = 930$ kg from these measurements, and is close to the theoretically estimated value of 0·012 m.

Since the calibration experiment contains no moment at the top surface, $M_2 = 0$, equation (18) allows h_2 to be derived from I_2 (unfortunately it is not possible to calibrate both I_2 and h_2). Taking $I_2 = 37{\cdot}9$ kg m^2 resulted in $h_2 \approx 0{\cdot}227$ m. This is 0·0175 m smaller than expected for $h_c = 0{\cdot}016$ m, which corresponds to the distance below the top surface at which the hammer excitation was located.

The effective mass calibration results are shown in Figure 11 as $20 \log_{10}(F_2 / m_2 \ddot{u}_2'')$ for $h_c = 0{\cdot}016$ m and $20 \log_{10}(F_2\, d_2 / I_2 \ddot{\theta}_2)$ for $h_2 = 0{\cdot}227$ m. Note that although the equivalent mass is effectively constant over the frequency range 40–800 Hz, the equivalent moment of inertia is only constant over the range 90–500 Hz. The deviation at low frequencies is

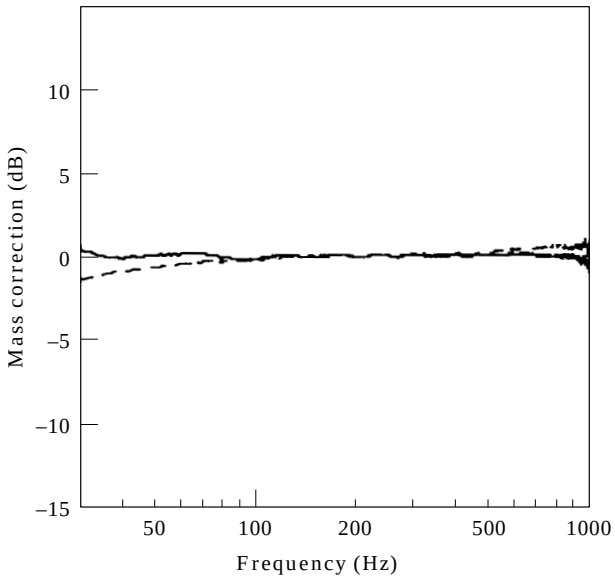

Figure 11. Equivalent mass (——) and moment of inertia (- - -) derived from measured transfer functions for hammer excitation expressed as a ratio to actual values assuming $h_c = 0{\cdot}016$ m and $h_2 = 0{\cdot}227$ m.

due to the resonances of the block on its springs, rather like the dip found in m_{eff} in the vertical direction (see Figure 7). For the lateral/rotational directions two such resonances occur, one dominated by translation of the block found at around 4·5 Hz, the other mainly rotation at around 13 Hz.

6.4. LATERAL AND ROTATIONAL MEASUREMENT RESULTS

The rotational stiffness measurements are presented here for only one vertical preload (40 kN). Compared to that of the vertical measurements the coherence was much less acceptable, necessitating the use of three or four sweeps over different frequency ranges with differing amplifier settings to achieve reasonable accuracy over the whole frequency range to be measured. Data with coherence less than 0·8 were rejected, which limited the frequency range to a maximum of 750 Hz.

Lateral excitation by a single exciter was via a thin rod to eliminate moment excitation of the block. Since the addition/subtraction devices cannot be used to output both the sum and the difference simultaneously, four measurements were carried out for each of the two force locations to give the transfer functions u_2'/u_1', θ_2/u_1', u_2'/θ_1 and θ_2/θ_1. Consequently the transfer function u_1/θ_1 (required in equation (24)) has not been measured directly. This has been reconstructed by using

$$\frac{u_1}{\theta_1} \approx \left(\frac{\theta_2}{\theta_1}\right) \Big/ \left(\frac{\theta_2}{u_1'}\right) + h_1 \qquad \text{for } \gamma^2_{\theta_2/\theta_1} \approx 1 \text{ and } \gamma^2_{\theta_2/u_1'} \approx 1, \tag{24}$$

although it would clearly be preferable to measure both quantities simultaneously.

The lateral and rotational stiffnesses ($k_{F,u}$ and $k_{M,\theta}$) are shown in Figure 12. It can be seen that, below about 100 Hz, the apparent magnitudes of both $k_{F,u}$ and $k_{M,\theta}$ increase with decreasing frequency. This is a result of "resonances" in the transfer functions (there are two peaks at low frequencies corresponding to the single peak found for the vertical direction in Figure 3), and is not a genuine stiffness of the pad, similar to the effect seen

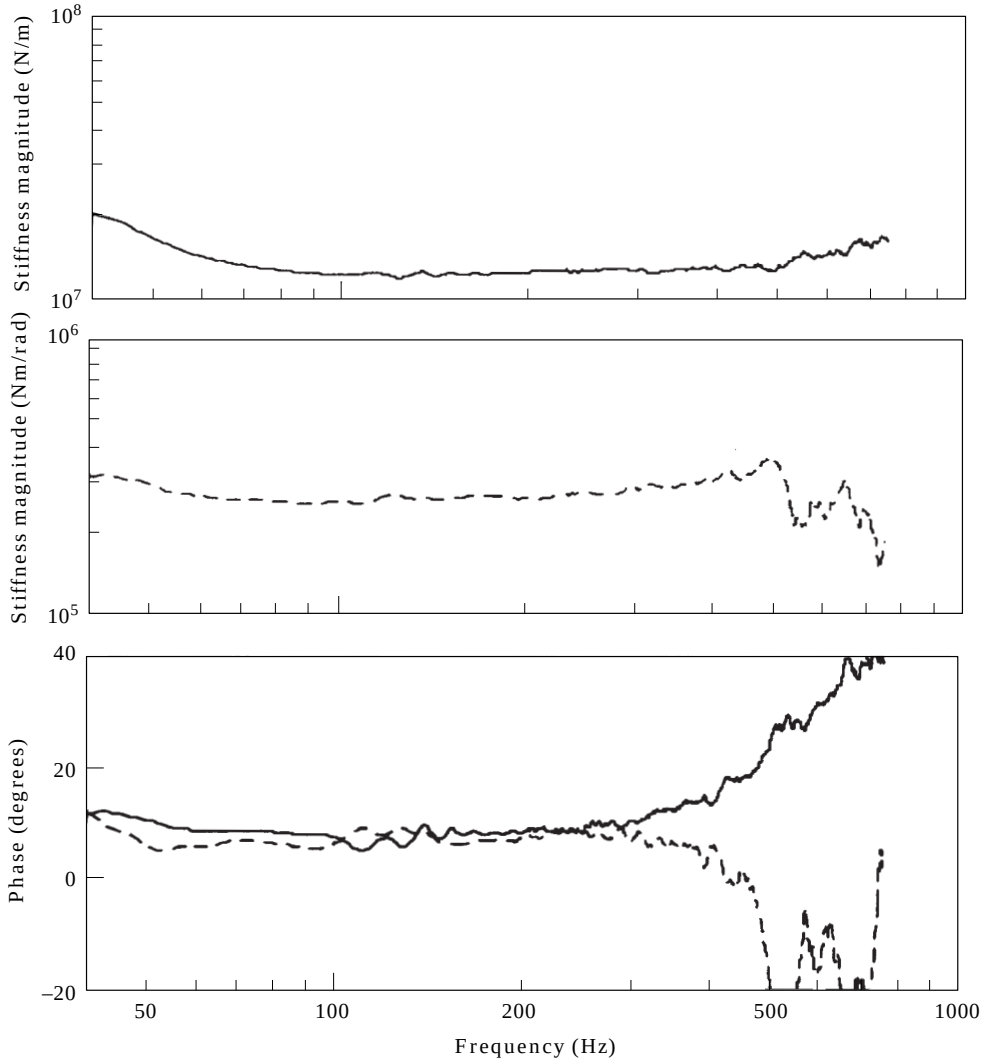

Figure 12. Magnitude and phase of complex lateral and rotational stiffness for 40 kN preload. ——, $k_{F,u}$; - - -, $k_{M,\theta}$.

in Figure 5. It is possible, in principle, to eliminate the effects of such "resonances" by measuring the differences $u_1 - u_2$ and $\theta_1 - \theta_2$ as in the vertical measurements. However this, and the frequency-dependent mass correction, have not been implemented for the lateral/rotational measurements here.

Above about 300 Hz, the phase of both $k_{F,u}$ and $k_{M,\theta}$ deviates from the low frequency behaviour, the former increasing strongly while the latter drops below 0. The stiffness magnitudes also deviate from those of the low frequency behaviour. This corresponds to frequencies where the cross terms $k_{F,\theta}$ and especially $k_{M,u}$ were found to have higher magnitudes. It is possible that internal resonances of the pad are responsible for the behaviour of the lateral stiffness—in the lateral direction such a resonance is expected at

roughly 1 kHz. However, it also reinforces the difficulty of obtaining reliable measurements in the lateral and rotational directions, as also found by the necessity for a lower coherence threshold than for the vertical direction.

As a check of the rotational stiffness, it should be possible to estimate the rotational stiffness from the vertical stiffness, approximating the pad as a homogeneous material, by using the relation

$$k_{M,\theta} \approx k_{vert} L^2/12, \tag{25}$$

where L is the width of the pad. When using a value of $L = 0{\cdot}154$ m (the width over the studs), the values calculated by using this equation agree extremely well with those measured directly (within an average of 1%). For other pads it would therefore be possible to estimate the rotational stiffness from the vertical stiffness in this way without needing to measure it directly. The method of this section would be needed, however, for the lateral stiffness.

7. CONCLUSIONS

The indirect method provides a reliable means of measuring the high frequency transfer stiffnesses of resilient elements in the low amplitude region as a function of frequency. This method is already being included in international standards. In this paper the dynamic behaviour of the measurement apparatus has been pointed out and extensions to the method have been described which allow a wider frequency range to be covered successfully. These involve deriving the compression of the resilient element by measuring the difference between accelerations above and below the element and correcting for the frequency dependence of the apparent mass of the lower block. A procedure has been successfully developed to allow the lateral and rotational components of stiffness to be separated.

ACKNOWLEDGMENTS

The measurements described here have been performed at TNO Institute of Applied Physics under contract to Chalmers University of Technology with funding provided by Abetong Teknik AB and the Swedish National Centre of Excellence CHARMEC.

REFERENCES

1. D. J. Thompson 1993 *Journal of Sound and Vibration* **161**, 421–446. Wheel-rail noise generation, part III: rail vibration.
2. D. J. Thompson and N. Vincent 1995 *Vehicle System Dynamics Supplement* **24**, 86–99. Track dynamic behaviour at high frequencies. Part 1: theoretical models and laboratory measurements.
3. ISO 10846-1 1997 Acoustics and vibration—Laboratory measurement of vibro-acoustic transfer properties of resilient elements—Part 1: principles and guidelines.
4. ISO 10846-2 1997 Acoustics and vibration—Laboratory measurement of vibro-acoustic transfer properties of resilient elements—Part 2: dynamic stiffness of elastic supports for translatory motion—direct method.
5. ISO/DIS 10846-3 1997 Acoustics and vibration—Laboratory measurement of vibro-acoustic transfer properties of resilient elements—Part 3: dynamic stiffness of elastic supports for translatory motion—indirect method.
6. U. J. Kurze 1994 *Acta Acustica* **2**, 483–490. Laboratory measurements of vibro-acoustical properties of resilient elements, Part I: theoretical basis.
7. J. W. Verheij 1980 *Proceedings of Inter Noise*, *Miami*, *Florida*, *U.S.A.*, 723–726. Measuring

sound transfer through resilient mountings for separate excitation with orthogonal translations and rotations.
8. J. W. VERHEIJ 1982 *Doctoral thesis*, *TNO Institute of Applied Physics*, *Delft*, *The Netherlands*. Multi-path sound transfer from resiliently mounted shipboard machinery.
9. D. J. THOMPSON and J. W. VERHEIJ 1997 *Applied Acoustics* **52**, 1–17. The dynamic behaviour of rail fasteners at high frequencies.
10. Å. FENANDER 1997 *Journal of Rail and Rapid Transit*, *Proceedings of I.Mech.E. part F* **211**, 51–62. Frequency dependent stiffness and damping of railpads.